

Comparison of the Dynamics of the Primary Events of Bacteriorhodopsin in Its Trimeric and Monomeric States

Jianping Wang, Stephan Link, Colin D. Heyes, and Mostafa A. El-Sayed

Laser Dynamics Laboratory, School of Chemistry and Biochemistry, Georgia Institute of Technology, Atlanta, Georgia 30332-0400 USA

ABSTRACT In this paper, femtosecond pump-probe spectroscopy in the visible region of the spectrum has been used to examine the ultrafast dynamics of the retinal excited state in both the native trimeric state and the monomeric state of bacteriorhodopsin (bR). It is found that the excited state lifetime (probed at 490 nm) increases only slightly upon the monomerization of bR. No significant kinetic difference is observed in the recovery process of the bR ground state probed at 570 nm nor in the fluorescent state observed at 850 nm. However, an increase in the relative amplitude of the slow component of bR excited state decay is observed in the monomer, which is due to the increase in the concentration of the 13-*cis* retinal isomer in the ground state of the light-adapted bR monomer. Our data indicate that when the protein packing around the retinal is changed upon bR monomerization, there is only a subtle change in the retinal potential surface, which is dependent on the charge distribution and the dipoles within the retinal-binding cavity. In addition, our results show that 40% of the excited state bR molecules return to the ground state on three different time scales: one-half-picosecond component during the relaxation of the excited state and the formation of the J intermediate, a 3-ps component as the J changes to the K intermediate where retinal photoisomerization occurs, and a subnanosecond component during the photocycle.

INTRODUCTION

Found in the purple membrane (PM) of *Halobacterium salinarium*, bacteriorhodopsin (bR) consists of a seven α -helical conformation within a single polypeptide chain of molecular weight ~ 27 kDa. As a light-driven proton pump, bR is the other type of photosynthetic center besides chlorophyll. Since its discovery, bR has served as the simplest model for studying bioenergetics for more than three decades (El-Sayed et al., 1981; Birge, 1981; Mathies et al., 1991; Ebrey, 1993; Lanyi, 1997).

Native bR is organized into a trimeric structure that is further organized into a two-dimensional hexagonal lattice with its atomic structure determined and refined with increasing resolutions in recent years (Henderson et al., 1990; Pebay-Peyroula et al., 1997; Essen et al., 1998; Luecke et al., 1998, 1999b; Edman et al., 1999). As a result of this, recent attention has been given to understanding the mechanism of the proton pump and the function of the internal bound water molecules and hydrogen-bonding network (Lanyi, 1999; Luecke et al., 1999a; Kandori et al., 2000; Wang and El-Sayed, 2001).

The unique purple color of bR ($\lambda_{\text{max}} = 568$ nm) in the visible absorption spectrum for the light-adapted (LA) state is due to the covalently bound all-*trans* retinal to the Lys-216 via a protonated Schiff base (Grigorieff et al., 1996;

Kimura et al., 1997). After light excitation, the excited state of bR rapidly relaxes from the all-*trans* to the 13-*cis* form with a quantum yield of $\sim 60\%$. The photocycle consists of a series of visible absorption spectrally distinguishable intermediates, including I, J, K, L, M₁, M₂, N, and O (Lozier et al., 1975; Lanyi and Varo, 1995). Proton release occurs during the L-M transition, whereas proton uptake occurs during the N-O transition, during which the retinal re-isomerization from 13-*cis* to all-*trans* occurs.

Subpicosecond pump-probe studies on native bR and its variants have been carried out extensively (Dinur et al., 1981; Nuss et al., 1985; Polland et al., 1986; Petrich et al., 1987; Mathies et al., 1988, 1991; Dobler et al., 1988; Song et al., 1993; Logunov et al., 1994, 1996; Haran et al., 1996; Hasson et al., 1996; Gai et al., 1998; Ye et al., 1999a,b). It is generally accepted that the bR excited state, I, relaxes in half a picosecond to form J, and J forms K in ~ 3 to 5 ps and that a near-infrared stimulated emission is observed during the same time window of the excited state relaxation. Recent resonance Raman results (Ye et al., 1999a) show that the retinal in K has the 13-*cis* form, suggesting that J has an all-*trans* form and thus the isomerization occurs during the J-K step.

This paper is focused on understanding the influence of the protein crystalline structure on the primary dynamics. In the trimeric structure of bR, intermonomer contacts are stronger between some helices than others. The structural stability of bR is dependent on many factors (Haltia and Freire, 1995), including intramolecular and intermolecular interactions, protein-lipid interactions (Subramaniam et al., 1993; Isenbarger and Krebs, 1999), and even protein-retinal interactions. Lipids play an important role in supporting the native hexagonal lattice. By weight, $\sim 25\%$ of PM are lipid

Submitted August 31, 2001, and accepted for publication May 9, 2002.

Jianping Wang's present address is Department of Chemistry, University of Pennsylvania, Philadelphia, PA 19104-6323.

Address reprint requests to Mostafa A. El-Sayed, Laser Dynamics Laboratory, School of Chemistry and Biochemistry, Georgia Institute of Technology, Atlanta, GA 30332-0400. Tel.: 404-894-0292; Fax: 404-894-0294; E-mail: mostafa.el-sayed@chemistry.gatech.edu.

© 2002 by the Biophysical Society

0006-3495/02/09/1557/10 \$2.00

molecules and the majority of them are polar due to their phosphate head groups.

It is known that by solubilizing the native trimeric bR fragments into nonionic detergent (e.g., Triton X-100), monomeric bR is formed (Dencher and Heyn, 1978; Dencher et al., 1983; Scherrer et al., 1989). Each bR molecule is individually capped inside the detergent micelle (Reynolds and Stoekenius, 1977), which replaces the native lipid surroundings. bR monomer is featured by the visible absorption spectrum with $\lambda_{\max} = 553$ nm, for the LA-bR monomer ($\lambda_{\max} = 568$ nm for trimer), and the monophasic Circular-dichroism (CD) band in the visible region (in contrast to the biphasic CD band for the trimer). In addition, the monomeric bR is less thermally stable than its native trimeric form (Brouillette et al., 1989). In the dark-adapted (DA) state of bR monomer, the isomeric ratio of (all-*trans*)/(13-*cis*) is determined to be 40/60 (Gonzalez-Manas et al., 1990), whereas in bR trimer it is close to 50/50, whereas in the LA state, this ratio is 95/5 for bR trimer (Song et al., 1995) and it varies from 65/35 to 85/15 for bR monomer (Gonzalez-Manas et al., 1990). These observations suggest that protein-protein, protein-lipids, and protein-retinal interactions influence the retinal configuration and the relative stability of its isomeric forms.

On the other hand, the photocycle of bR monomer is qualitatively the same as bR trimer (Dencher et al., 1983; Fukuda et al., 1990; Milder et al., 1991), except that the lifetimes of the L and N intermediates are significantly shorter in the monomer (Dencher and Heyn, 1982; Varo and Lanyi, 1991). This indicates that the crystalline structure of bR may affect the kinetics and energetics of the bR photocycle (Varo and Lanyi, 1991). Yet, it is still unknown whether or not changing the lattice structure and protein aggregation state influence the dynamics of the ultrafast primary events upon photoexcitation. In addition, one of the reasons that makes the study of the trimeric structure versus the monomeric structure of bR interesting is that the recent x-ray crystallographic studies are based on the crystallization of bR in the cubic lipid phase following detergent solubilization (Landau and Rosenbusch, 1996; Luecke et al., 1999b) by which the conformation of bR might be different from the native state.

In the present study, femtosecond transient visible pump-probe spectroscopy has been used to examine the dynamics of retinal in the bR excited state, the rate of excited state relaxation, and of the early photointermediates transitions for the native trimeric state and the Triton X-100 solubilized monomeric state. The influence of the protein aggregation state and protein lattice structure on the primary processes and photocycle kinetics of bR are examined and discussed.

MATERIALS AND METHODS

Native bR in purple membrane was prepared from the *Halobacterium salinarium* strain ET1001 as described previously (Oesterhelt and Stoek-

enius, 1971). PM fragments in the form of the trimeric state is dispersed in 25 mM K_2HPO_4 buffer, pH ~ 7.0 . Monomeric bR was prepared by solubilizing native bR suspension in Triton X-100, according to previously described procedures (Dencher and Heyn, 1982; Kovacs et al., 1995). Briefly, PM suspension in 25 mM K_2HPO_4 buffer, pH ~ 7.0 was mixed with Triton X-100 (Aldrich, St Louis, MO) at a ratio of 1:7 (w/w). The mixture was kept in the dark for at least 48 h. Successful solubilization of bR monomer in Triton X-100 is indicated by the fact that no sediment occurs after 30-min centrifugation at $45,000 \times g$, and the shift in the absorption spectrum maximum from 568 to 553 nm. The concentration of bR samples was controlled to give optical density of ~ 1.0 at their maximal absorption wavelength in a 2-mm quartz cuvette. All spectroscopic measurements were carried out at room temperature. Samples were light adapted for 30 min before each pump-probe experiment.

Ultraviolet-Visible absorption spectra were taken by using a 3101PC UV-Vis spectrometer (Shimadzu, Columbia, MD). CD spectra were taken by using a Jasco J-720 spectropolarimeter (Japan Spectroscopic Co., Ltd, Tokyo, Japan). Flash photolysis measurements were carried out by using a system consisting of a MOPO (Spectral Physics) for laser excitation at 560 nm (10 ns, 10 Hz); a Xenon lamp was used for continuous probing, in combination with a monochromator and photomultiplier tube, and a 500-MHz transient digitizer (9350A, LeCroy, Chestnut Ridge, NY). The M kinetics were measured by probing absorption at 412 nm with 600 to 1000 laser shots averaged.

Femtosecond pump-probe spectroscopy system has been described previously (Logunov et al., 2001; Burda et al., 2000). Briefly, an amplified Ti:sapphire laser system (CPA 1000, Clark MXR, Dexter, MI) was pumped by a diode-pumped, frequency-doubled Nd:Vandate laser (Verdi, Coherent, Palo Alto, CA). This produced laser pulses of 100 fs duration (full width at half maximum) with the energy of 1 mJ at 800 nm. The repetition rate was 1 kHz. A small part (4%) of the fundamental generated a white light continuum in a 1-mm sapphire plate, which was used as the probe light. The remaining laser light was split into two equal parts to pump two identical OPAs (TOPAS, Quantronix, East Setauket, NY), which produced signal and idler waves with a total energy of 120 μ J. Tunable wavelengths in the visible range were then produced by SHG and SFG of the signal wave. Alternatively, one part of the fundamental output could be frequency-doubled in a beta borium borate crystal to generate a 400-nm pump beam instead of pumping the OPA. The excitation beam was modulated by an optical chopper with a frequency of 500 Hz. The probe light was split into a signal and a reference beam. After passing the monochromator (Acton Research, Acton, MA) both beams were detected by two photodiodes (Thorlab, Newton, NJ). The kinetic traces were obtained using a sample-and-hold unit and a lock-in-amplifier (Stanford Research Systems, Sunnyvale, CA). The time-dependent spectra were recorded by a system consisting of monochromator and nitrogen-cooled CCD camera (Princeton Instruments, Monmouth Junction, NJ). The chirp of the white light continuum was corrected for the transient spectra.

RESULTS AND DISCUSSION

Steady-state visible absorption spectra and CD spectra have been compared for the light-adapted bR in the form of its native trimeric state and Triton X-100 solubilized monomeric state, as shown in Fig. 1 A. A large blue shift (from 568–553 nm) is observed in the absorption maximum from bR trimer to monomer in the retinal absorption spectra. There are two reasons for this blue shift: one is due to the difference in the retinal isomer composition in these two states. The retinal isomer compositions and absorption maxima (λ_{\max}) have been listed in Table 1. It has been determined (Gonzalez-Manas et al., 1990) that the concentration of all-*trans* decreases from 94% to as low as 84% as bR

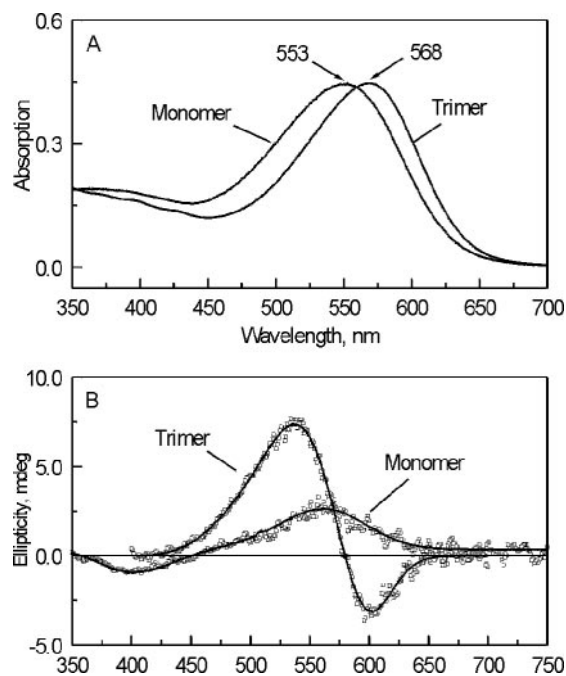


FIGURE 1 Visible absorption spectra (350–700 nm) and CD spectra of retinal in the LA bR in the form of the native trimeric state and in the Triton X-100 solubilized monomeric state. (A) A 15-nm blue shift is shown in the absorption maximum (λ_{\max}) from the trimer to monomer; (B) A band shape change from the biphasic to monophasic in the CD spectra is shown to occur from the trimer to monomer.

becomes monomerized (0.01 M Triton X-100) under the LA condition. However, this blue shift cannot be solely due to the isomer composition change in these two states, because for example, the dark-adapted state of bR trimer has its λ_{\max} shifted to 560 nm when the (all-*trans*) decreases to 45%. In addition, the DA- monomer has its λ_{\max} further shift to 546 nm in which (all-*trans*)/(13-*cis*) becomes 40/60 (Gonzalez-Manas et al., 1990), similar to that in the DA-trimer. There-

TABLE 1 Retinal chromophore isomeric composition and absorption maximum (λ_{\max}) for the native trimeric state and Triton X-100 solubilized monomeric state in the LA and DA conditions at room temperature

| Sample | Isomer composition (%) | | λ_{\max} (nm)* |
|-------------------------|------------------------|----------------|------------------------|
| | All- <i>trans</i> | 13- <i>cis</i> | |
| LA-trimer [†] | 94 | 6 | 568 |
| DA-trimer [‡] | 45 | 55 | 560 |
| LA-monomer [†] | 84 | 16 | 553 |
| DA-monomer [‡] | 40 | 60 | 546 |

*The λ_{\max} of DA-trimer and monomer were measured after 2-h DA from their LA forms.

[†]Isomer ratio data are taken from a previous result at pH 6 (Song et al., 1995).

[‡]Isomer ratio data are taken from a previous result at 20 mM Tris buffer, pH 5 (Gonzalez-Manas et al., 1990).

Experimental conditions: 25 mM K_2HPO_4 buffer, pH \sim 7.

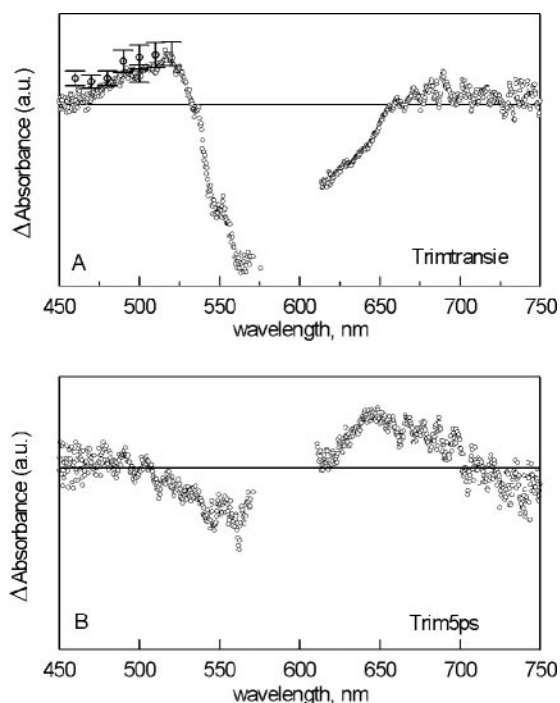


FIGURE 2 Transient absorption spectra of light-adapted bR trimer at different time delay after excitation with 100-fs laser pulse: (A) 0.0 ps; (B) 3.8 ps. The profile of the absorption band between 450 and 520 nm was also obtained from wavelength-dependent kinetics measurement.

fore, the most important reason for the blue shift of retinal absorption in the monomer is the environmental changes of the retinal binding site, as has been seen in many other cases, e.g., the mutation of the Schiff base proton acceptor Asp-85 to a neutral group shifts the retinal absorption maximum to 604 nm (Song et al., 1993).

In the CD spectra shown in Fig. 1 B, retinal shows an asymmetric biphasic CD band in the trimeric state, consisting of a positive band at \sim 540 nm and a negative band at \sim 600 nm. In the monomeric state, only a monophasic CD band is present with its maximum at \sim 555 nm, which is an indicator of losing the native trimeric structure. The biphasic CD band in bR trimer has been attributed originally to the existence of the retinal exciton coupling between the chromophores in the trimer structure of bR (Heyn et al., 1975; Becher and Cassim, 1977; Muccio and Cassim, 1979) and later was proposed to originate from the existence of retinal environmental heterogeneity (El-Sayed et al., 1989; Jang et al., 1990; Wu and El-Sayed, 1991). Thus, the change in the CD band shape from the biphasic to monophasic is due to the loss of either the exciton coupling or to the change in the heterogeneity as a result of detergent solubilization. This indicates that retinal does feel a different binding environment as a result of loss of the trimeric form within the detergent micelle. This is in agreement with the visible absorption spectral change shown in Fig. 1 A.

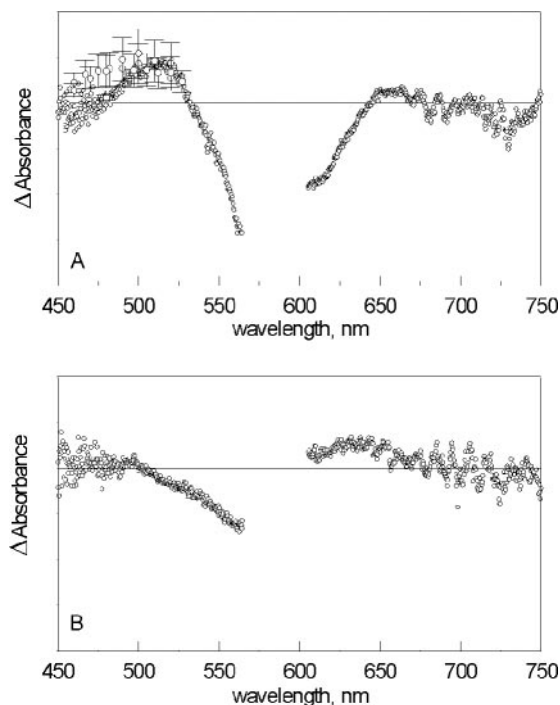


FIGURE 3 Transient absorption spectra of light-adapted, Triton X-100 solubilized bR monomer at different time delay after excitation with 100-fs laser pulse: (A) 0.0 ps; (B) 3.8 ps. The profile of the absorption band between 450 and 520 nm was also obtained from wavelength-dependent kinetics measurement.

We would like to know the influence of the retinal environment change on the dynamics of the primary events in bR. Fig. 2 shows the transient absorption spectra of LA-bR trimer at two delay times after the 100-fs pulsed laser excitation in the spectral region of 450 to 750 nm. The retinal in the bR excited state is characterized by an absorption band that is blue shifted (490 nm) from the ground state bleach band (568 nm). It also shows the first intermediate formation (J, $\lambda_{\max} = 625$ nm, Fig. 2 A), and transition from J to K ($\lambda_{\max} = 610$ nm, Fig. 2 B). These results are in general agreement with previous results (Sharkov et al., 1985; Kobayashi et al., 1991; Mathies et al., 1988; Hasson et al., 1996; Logunov et al., 1996, 1998).

The intensity of the continuum generated with 800-nm light drops off sharply around 470 nm in our setup, which will influence the spectral shape of the excited state absorption. However, using the more sensitive lock-in technique we tried to map out the excited state absorption band more clearly by measuring the single-wavelength kinetics in that spectral region. The results are superimposed in the figures and show that the absorption profile of the trimer and monomer is similar within experimental errors. Due to the limitations in this spectral regime a precise determination of the excited state maximum is not possible at the present time. To do this, one may need to deconvolute the transient

TABLE 2 Kinetics parameters of the excited state relaxation and ground state recovery for the native trimeric state and Triton X-100 solubilized monomeric state in the LA conditions

| Sample | Lifetime (amplitude) | | λ (nm) | |
|----------------------------|----------------------|-------------------|----------------|------|
| | τ 1, ps (A1) | τ 2, ps (A2) | Probe | Pump |
| Trimer (490) | 0.46 (>95%) | — | 490 | 555 |
| Monomer (490) | 0.63 (87%) | 3.51 (13%) | 490 | 555 |
| Trimer (850) | 0.44 (>95%) | — | 850 | 555 |
| Monomer (850) | 0.55 (90%) | 3.45 (10%) | 850 | 555 |
| Trimer (550)* | 0.57 (65%) | 3.08 (21%) | 550 | 580 |
| Monomer (540) [†] | 0.65 (68%) | 4.61 (18%) | 540 | 555 |

*[†], Ground state bleach recovery has a rather long component, which takes ~10 to 15% of the overall amplitude for both the trimer and monomer. Experimental conditions: 25 mM K_2HPO_4 buffer, pH ~7.

spectrum for the ground state bleach that overlaps with the excited absorption.

In the case of solubilized monomer, the transient absorption spectra of the LA-monomer at two delay times are shown in Fig. 3. A very similar transient spectral change is observed in monomerized bR compared with native bR. Three major contributions are shown in the spectral region from 450 to 750 nm: changes in the excited state absorption (blue shifted from the ground state absorption, Fig. 3 A), ground state bleach, and photointermediates (J and K) absorption (red shifted in respect with the ground state absorption; Fig. 3 B). By comparing Figs. 2 and 3, it is noticed that there is almost no difference in the bR excited state absorption profile. However, a slight blue shift of the K intermediate absorption is observed in bR monomer at 3.8-ps delay time, in agreement with the result that bR monomer has its center frequency blue shifted in the linear absorption spectrum (Fig. 1 A). Detailed kinetics comparison of these three absorption and bleach bands shows similar lifetimes in the native trimeric state and in the solubilized monomeric state (Table 2).

Fig. 4 compares the decay of the excited state for the native trimer and the solubilized monomer. It is observed that the excited state of trimeric bR has a major relaxation process with lifetime of 0.46 ps (95%), whereas that of monomeric bR has two relaxation components with lifetimes and relative amplitudes of 0.63 (87%) and 3.51 ps (13%), respectively. The 0.46-ps decay time for the trimer is in good agreement with that reported elsewhere (Mathies et al., 1988; Song et al., 1993; Hasson et al., 1996; Logunov et al., 1996). This indicates the transition time from bR-excited state to the J photointermediate (λ_{\max} at 625 nm). The only major half-picosecond component in the trimer is associated with the fact that it has more than 94% of all-*trans* retinal. As the retinal isomeric ratio changes, the excited state may have more than one decay processes each with significant relative amplitudes, as seen in deionized bR and mutants (Song et al., 1993, 1996; Hasson et al., 1996; Logunov et al., 1996). The deionized bR has 1:1 mixture of all-*trans* and 13-*cis* in its LA form (Song et al., 1995) and

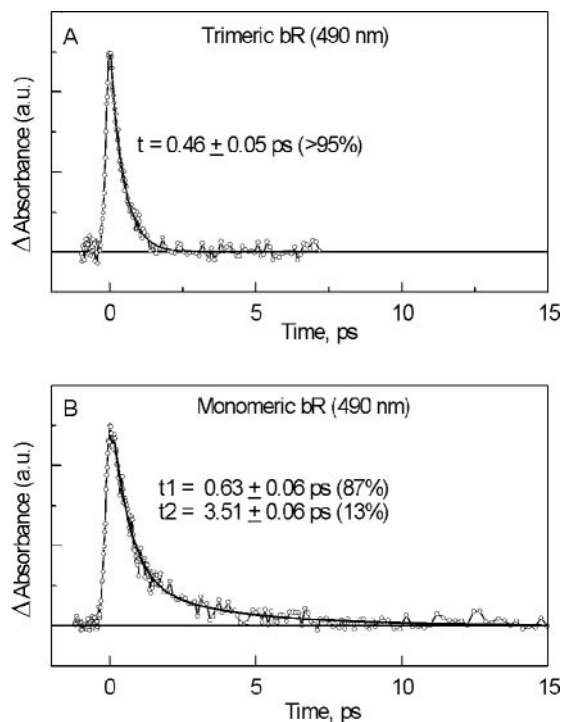


FIGURE 4 Comparison of the bR excited state absorption relaxation on at 490 nm for (A) bR trimer and (B) bR monomer. The lifetimes and their relative ratios were also given in each case. A small difference is observed between the trimeric and monomeric bR.

the excited state of deionized bR decays with two components weighted almost equally in their relative amplitudes, indicating that each isomer has different excited state relaxation times. This is also the case of monomeric bR with the estimation of the relative amplitude ratio of the fast and slow component (87/13), fairly close to the *trans*-to-*cis* ratio shown in Table 1 for the LA-monomer (84/16). Therefore, we assign the fast component (0.63 ps) to the relaxation of all-*trans* retinal and the slow component (3.51 ps) to the relaxation of 13-*cis* form. Considering the steady-state visible absorption spectra shown in Fig. 1, it seems that by breaking the membrane crystalline hexagonal lattice and destroying the trimer structure, the content of the all-*trans* decreases, which causes a decrease in the overall photocycle efficiency and in the proton pump yield. This is because for a given number of bR molecules, the 13-*cis* form does not go through the photocycle as all-*trans* form and does not pump protons.

Most important, comparing the fast relaxation of bR excited state in the monomer to that in the trimer, one notices that the fast lifetime change from the trimer to monomer is not significant. It shows a slight increase from 0.46 ps in the trimer to 0.63 ps in the monomer, however, both still falls in the half picosecond regime (0.5 ± 0.1 ps). In other words, breaking the trimeric structure of native bR, the excited state lifetime is not kinetically influenced. This

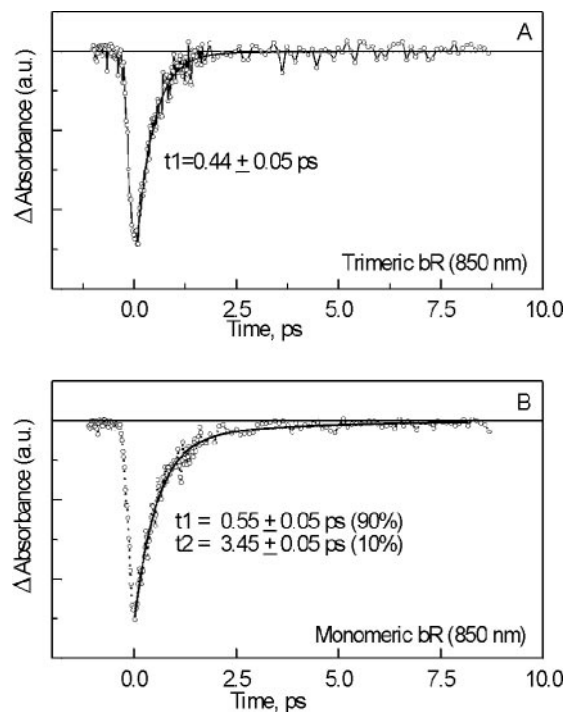


FIGURE 5 Comparison of the stimulated emission monitored at 850 nm for (A) bR trimer and (B) bR monomer. The lifetimes and their relative ratios were also given in each case. A small difference in the lifetimes of the stimulated emission was observed in the monomeric bR in agreement with that shown in Fig. 4.

indicates that the trimer structure does not have a significant catalytic effect on the primary photo-events of bR. However, major catalysis influence on the retinal excited state lifetime is found when there is a significant change inside the protein. For example, by mutating only one amino acid group (such as Asp-85), the rate of retinal photoisomerization drops to 1/20 of the native bR (Song et al., 1993).

Because it is generally believed that a fluorescent state that gives a stimulated emission in the near infrared region can be used to characterize the lifetime of the bR excited state, we have compared the results of the trimer and monomer in this region. The lifetime of this fluorescent state is usually found to be approximately one-half picosecond, which represents the I- to J- transition (Polland et al., 1984; Dobler et al., 1988; Mathies et al., 1988). The kinetics of the stimulated emission at 850 nm for these two forms of bR is shown in Fig. 5. As can be seen that in bR trimer, the stimulated emission relaxes with a major exponential component of 0.44 ps, fairly close to that of the excited state absorption relaxation time shown in Fig. 4 (0.46 ps). In the case of the monomer, the emission relaxes with two components (0.55 and 3.5 ps). From 0.44 to 0.55 ps, the time constant of the emission state is only slightly longer in the monomer but within the regime of 0.5 ± 0.05 ps. This confirms our conclusion that the excited state relaxation is only slightly slower in bR monomer, presumably the emis-

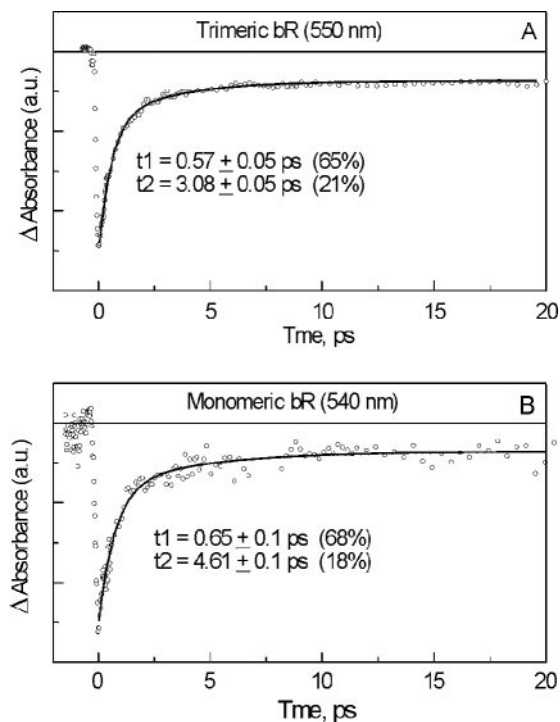


FIGURE 6 Comparison of the recovery of bR ground state absorption for (A) bR trimer at 550 nm and (B) bR monomer at 540 nm. A general elongation of the lifetimes were shown in bR monomer than trimer. Note that there is always an extremely long-lived component (80 ps) that accounts for $\sim 15\%$ of the whole amplitude.

sion at 850 nm provide a more reasonable measure of the bR excited state. The stimulated emission was also probed at longer wavelength, e.g., 950 nm, similar results were found (not shown here). In summary, it is shown that from the trimeric to the monomeric bR, the excited state lifetime is no more than 25% different.

We also examined the ground state recovery process. The ground state recovery shows two exponential component processes in bR trimer (Fig. 6 A) with their lifetimes and relative amplitudes of 0.57 (65%) and 3.07 ps (21%) and a rather long component (80 ps). This is generally seen in native bR, whose ground state is repopulated although a process with multicomponents (Mathies et al., 1988; Logunov et al., 1996). In the monomerized form (Fig. 6 B), the first two components become 0.65 (68%) and 4.61 ps (18%), showing only a slightly change in both the lifetime and relative amplitude. The change in the fast component lifetime from trimer to monomer (0.57 vs. 0.65 ps) is in the same trend to that observed in the excited state absorption relaxation (0.47 vs. 0.63 ps), and also to that of the fluorescent state relaxation (0.46 vs. 0.55 ps). This indicates clearly that the dynamics of the primary events in bR is influenced only slightly by converting the trimeric state into the solubilized monomeric state.

The question of whether the photoisomerization of the retinal occurs in the 0.5-ps time domain was raised recently

based on different results by using atomic force sensing technique (Rouso et al., 1997), visible pump-probe spectroscopy (Zhong et al., 1996; Ye et al., 1999a), and time-resolved Raman spectroscopy (Atkinson et al., 2000). A model has been proposed in which a conical intersection was proposed for the retinal photoisomerization (Garavelli et al., 1997; González-Luque et al., 2000). More recently it is proposed (Logunov et al., 2001) that the excited state relaxes first to a minimum on the excited state potential energy surface on the 0.5-ps time scale to give J as proposed originally by Atkinson et al. (2000) from which J isomerizes through conical intersection to form K. The question now arises as to when the 40% of the excited state molecules return to the ground state? From the above results, it seems that the majority ($\sim 65\%$) returns during the I to J process and $\sim 20\%$ returns to the ground state from the conical intersection, i.e., during the K formation.

Fig. 7 shows the absorption kinetics probed at 660 nm for both trimer and monomer. In the early time domain, a rapid bleach signal is observed, due to either the edge of the ground state bleach signal or the stimulated emission in this region, as previously suggested (Ye et al., 1999a). This bleach band turns into an absorption band with a rise time of 160 to 200 fs for both trimer and monomer (shown in Fig. 7, A and C). This is shorter than the J formation, which could be due to the ground state bleach recovery having opposite sign for the intensity change. The relaxation of the absorption shows a 3-ps component, which is an indicator of the J to K transition (Fig. 7, B and D).

From the above results, it is suggested that the primary molecular dynamics of bR is not heavily dependent on the aggregation state or on the crystalline lattice structure, and hence suggesting that the photoisomerization of retinal is not significantly influenced by the helix-helix interactions or the helix-lipids interactions and/or even helix-retinal interactions. It is those interactions that keep bR molecular integrity. However, the retinal environment inside the protein, especially charge distributions, affect the photoisomerization rate substantially as reported before (Song et al., 1993).

Previous studies have also shown that, in general, the photocycle dynamics are not significantly affected by detergent solubilization (Varo and Lanyi, 1991), except in the L-M and N-O transitions. Indeed, our results in Fig. 8 shows that the formation time of the M intermediate is ~ 10 times faster in the monomer (1 μ s (10%) and 6 μ s (90%), curve a) than that in the trimer (15 μ s (37%) and 64 μ s (63%), curve c). This is in good agreement with previous reports (Dencher and Heyn, 1982; Varo and Lanyi, 1991). The formation of M is in the time regime that a proton is transferred from the retinal Schiff base to the proton acceptor Asp-85, whereas another proton is released onto the surface (Liu, 1990; Rammelsberg et al., 1998). The M formation is proposed to be rate determined by the protein conformation changes during this process (Dupuis et al.,

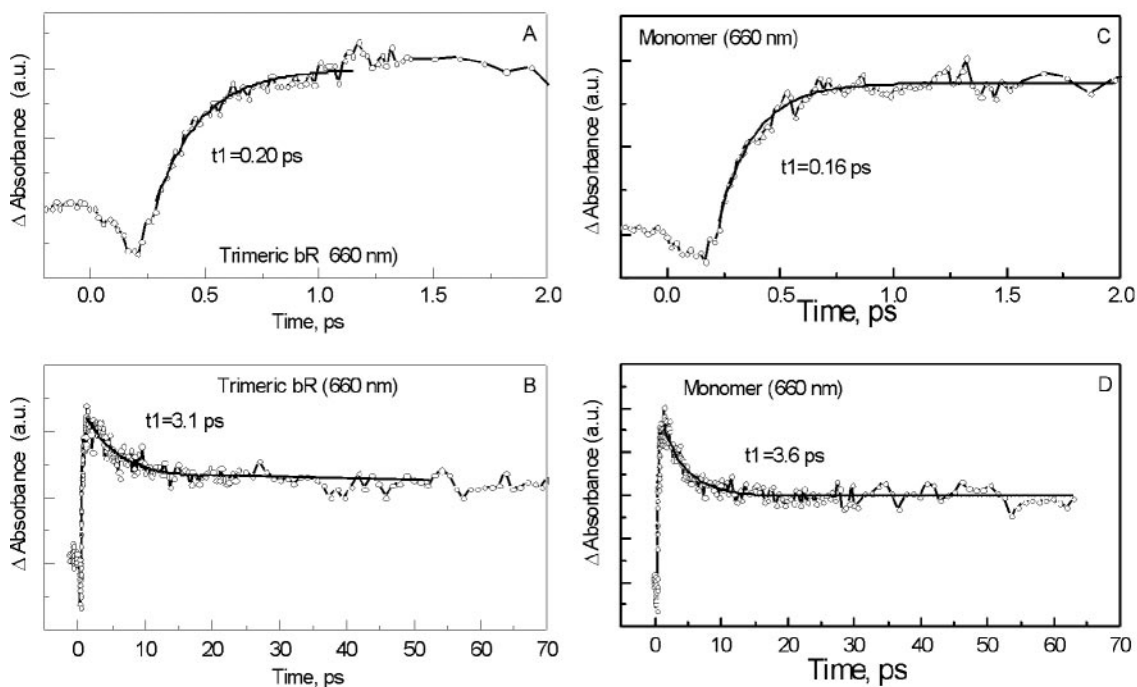


FIGURE 7 Absorption kinetics at 660 nm for the trimeric bR and monomeric bR, showing the formation of the J intermediate and J to K transition. (A and B) bR trimer; (C and D) bR monomer.

1985). These processes are expected to be dependent on the protein environment of the lattice structure and its lipid composition. By washing out the detergent through long time dialysis, one can restore its aggregation state partially to form the “oligomer” state. The formation of the oligomeric bR, indeed, shows a decrease in the lifetime of the signal (curve b), having 11 μs (85%) and 49 μs (15%). This suggests that protein aggregation state is very important in controlling the photocycle kinetics. The acceleration of the M formation in the monomer might reflect an increase in response to the change in protein conformation as a result of the fact that in the monomerized state, each individual bR molecule has a much more flexible secondary structure and

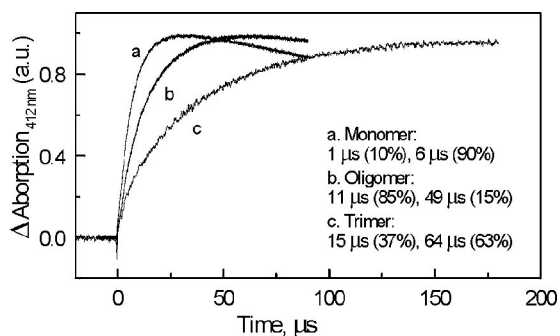


FIGURE 8 M formation kinetics of bR in bR monomeric state (a); in the partially detergent-removed “oligomer” state (b); and in the native trimeric state (c). Curve fitting of M formation kinetics shows a biexponential process with their time constants and relative amplitudes shown.

therefore a relatively large number of conformational states than that in the rigid, fixed trimer state present in the native structure. However, one disadvantage of the flexibility is it gives rise to protein instability. Our recent results have shown that retinal binding and protein secondary structure is much less stable in solubilized monomeric bR (Wang et al., 2002). On the other hand, one could imagine that the protein conformation of the photointermediates in the trimer would be more ordered than those in the bR monomer, which might be one of the reasons nature keeps this proton pump and photocycle machinery in a well defined allosteric pathway. In addition, from the formation of the K intermediate (a few ps) to the formation of the M intermediate (a few tens of microseconds), the photoexcitation energy originally stored in retinal is transferred from the retinal to the protein, and yet protein conformational adjustment occurs very slowly.

The trimeric unit of bR is the tertiary structure selected by nature. The tertiary structure of bR is dependent on the hydrophobic packing at specific protein-protein and protein-lipid interfaces within the membrane bilayer (Krebs et al., 1997). Such a protein-protein interaction is illustrated in Fig. 9. A rather close interface is shown in between helices B and D, whose contribution in stabilizing membrane lattice has been recognized recently. For example, a single amino acid substitution in the helix-D is sufficient to disrupt the crystal lattice (Krebs et al., 1997).

The photoisomerization of retinal protonated SB is a lot faster in the protein than in other media (Schoelein et al.,

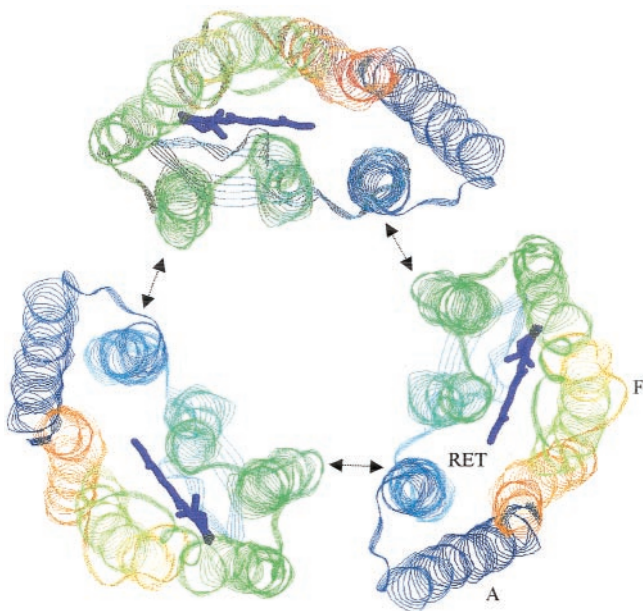


FIGURE 9 View of the bR trimeric structure to show the helical-helical interactions, helical retinal interactions in bR trimer, especially between helices B and D. There is also helical-lipid interactions that were not shown here.

1991; Mathies et al., 1988), which leads to the catalytical role of the surrounding protein (Ebrey, 1993; Song et al., 1993). Because the half-picosecond component of the excited lifetime is not significantly affected when changing protein packing patterns and that this component is responsible for the I to J conversion, and the latter is then associated with the all-*trans* to 13-*cis* isomerization, it is reasonable to conclude that destroying protein trimeric structure via nonionic detergent solubilization does not affect much of the photoisomerization of retinal chromophore. However, protein tertiary and secondary structural change from trimer to monomer results in molecular dynamics change in the microsecond to millisecond photocycle kinetics that are associated with the large protein conformational reorganization on the time scale of the proton release and uptake events. Our results show that the trimer structure and the lipids do not have a major effect in determining the charge distribution that controls the potential energy surface on which the excited state of retinal relaxes.

The authors thank the Chemical Sciences, Geosciences, and Biosciences Division, Office of Basic Energy Sciences, Office of Sciences, U.S. Department of Energy (under Grant DE-FG02-97ER14799) for financial support. We thank Dr. Loren Williams for allowing us to use the CD spectropolarimeter.

REFERENCES

- Atkinson, G. H., L. Uji, and Y. Zhou. 2000. Vibrational Spectrum of the J-625 intermediate in the room temperature Bacteriorhodopsin photocycle. *J. Phys. Chem. A* 104:4130–4139.
- Becher, B., and J. Y. Cassim. 1977. Effects of bleaching and regeneration on the purple membrane structure of *Halobacterium halobium*. *Biophys. J.* 19:285–297.
- Birge, R. R. 1981. Photophysics of light transduction in rhodopsin and bacteriorhodopsin. *Annu. Rev. Biophys. Bioeng.* 10:315–354.
- Brouillette, C. G., R. B. McMichens, L. J. Stern, and H. G. Khorana. 1989. Structure and thermal stability of monomeric bacteriorhodopsin in mixed phospholipid/detergent micelles. *Proteins Struct. Funct. Genet.* 5:38–46.
- Burda, C., M. H. Abdel-Kader, S. Link, and M. A. El-Sayed. 2000. Femtosecond dynamics of a simple merocyanine dye: does deprotonation compete with isomerization? *J. Am. Chem. Soc.* 122:6720–6726.
- Dencher, N. A., and M. P. Heyn. 1978. Solubilization of purple membrane by the non-ionic detergents Triton X-100 and octyl- β -D-glucoside. *Dev. Halophilic Microorg.* 1:233–238.
- Dencher, N. A., and M. P. Heyn. 1982. Preparation and properties of monomeric bacteriorhodopsin. *Methods Enzymol.* 88:5–10.
- Dencher, N. A., K. D. Kohl, and M. P. Heyn. 1983. Photochemical cycle and light-dark adaptation of monomeric and aggregated bacteriorhodopsin in various lipid environments. *Biochemistry.* 22:1323–1334.
- Dinur, U., B. Honig, and M. Ottolenghi. 1981. Analysis of primary photochemical processes in bacteriorhodopsin. *Photochem. Photobiol.* 33: 523–527.
- Dobler, J., W. Zinth, W. Kaiser, and D. Oesterheld. 1988. Excited-state reaction dynamics of bacteriorhodopsin studied by femtosecond spectroscopy. *Chem. Phys. Lett.* 144:215–220.
- Dupuis, P., T. C. Corcoran, and M. A. El-Sayed. 1985. Importance of bound divalent cations to the tyrosine deprotonation during the photocycle of bacteriorhodopsin. *Proc. Natl. Acad. Sci. U. S. A.* 82: 3662–3664.
- Ebrey, T. G. 1993. Light energy transduction in bacteriorhodopsin. CRC Press, New York.
- Edman, K., P. Nollert, A. Royant, H. Belrhali, E. Pebay-Peyroula, J. Hajdu, R. Neutze, and E. Landau. 1999. High-resolution X-ray structure of an early intermediate in the bacteriorhodopsin photocycle. *Nature.* 401: 822–826.
- El-Sayed, M. A., B. Karvaly, and J. M. Fukumoto. 1981. Primary step in the bacteriorhodopsin photocycle: photochemistry or excitation transfer? *Proc. Natl. Acad. Sci. U. S. A.* 78:7512–7516.
- El-Sayed, M. A., C. T. Lin, and W. R. Mason. 1989. Is there an excitonic interaction or antenna system in bacteriorhodopsin? *Proc. Natl. Acad. Sci. U. S. A.* 86:5376–5379.
- Essen, L. O., R. Siegert, W. D. Lehmann, and D. Oesterheld. 1998. Lipid patches in membrane protein oligomers: crystal structure of the bacteriorhodopsin-lipid complex. *Proc. Natl. Acad. Sci. U. S. A.* 95: 11673–11678.
- Fukuda, K., A. Ikegami, A. Nasuda-Kouyama, and T. Kouyama. 1990. Effect of partial delipidation of purple membrane on the photodynamics of bacteriorhodopsin. *Biochemistry.* 29:1997–2002.
- Gai, F., K. C. Hasson, J. C. McDonald, and P. A. Anfinsen. 1998. Chemical dynamics in proteins: the photoisomerization of retinal in bacteriorhodopsin. *Science.* 279:1886–1891.
- Garavelli, M., P. Celani, F. Bernardi, M. A. Robb, and M. Olivucci. 1997. The C5H6NH₂⁺ protonated Schiff base: an ab initio minimal model for retinal photoisomerization. *J. Am. Chem. Soc.* 119:6891–6901.
- González-Luque, R., M. Garavelli, F. Bernardi, M. Merchán, M. A. Robb, and M. Olivucci. 2000. Computational evidence in favor of a two-state, two-mode model of the retinal chromophore photoisomerization. *Proc. Natl. Acad. Sci. U. S. A.* 97:9379–9384.
- Gonzalez-Manas, J. M., G. Montoya, C. Rodriguez-Fernandez, J. I. G. Gurtubay, and F. M. Goni. 1990. The interaction of Triton X-100 with purple membrane: effect of light-dark adaptation. *Biochim. Biophys. Acta.* 1019:167–169.
- Grigorieff, N., T. A. Ceska, K. H. Downing, J. M. Baldwin, and R. Henderson. 1996. Electron-crystallographic refinement of the structure of bacteriorhodopsin. *J. Mol. Biol.* 259:393–421.
- Haltia, T., and F. Freire. 1995. Forces and factors that contribute to the structural stability of membrane proteins. *Biochim. Biophys. Acta.* 1228: 1–27.

- Haran, G., K. Wynne, A. Xie, Q. He, M. Chance, and R. M. Hochstrasser. 1996. Excited state dynamics of bacteriorhodopsin revealed by transient stimulated emission spectra. *Chem. Phys. Lett.* 261:389–395.
- Hasson, K. C., F. Gai, and P. A. Anfinsen. 1996. The photoisomerization of retinal in bacteriorhodopsin: experimental evidence for a three-state model. *Proc. Natl. Acad. Sci. U. S. A.* 93:15124–15129.
- Henderson, R., J. M. Baldwin, T. A. Ceska, F. Zemlin, E. Beckmann, and K. H. Downing. 1990. An atomic model for the structure of bacteriorhodopsin. *Biochem. Soc. Trans.* 18:844.
- Heyn, M. P., P. J. Bauer, and N. A. Dencher. 1975. A Natural CD label to probe the structure of the purple membrane from *Halobacterium halobium* by means of exciton coupling effects. *Biochem. Biophys. Res. Commun.* 67:897–903.
- Isenbarger, T. A., and M. P. Krebs. 1999. Role of helix-helix interactions in assembly of the Bacteriorhodopsin lattice. *Biochemistry.* 38: 9023–9030.
- Jang, D. J., M. A. El-Sayed, L. J. Stern, T. Mogi, and H. G. Khorana. 1990. Sensitivity of the retinal circular dichroism of bacteriorhodopsin to the mutagenetic single substitution of amino acids: tyrosine. *FEBS Lett.* 262:155–158.
- Kandori, H., N. Kinoshita, Y. Yamazaki, A. Maeda, Y. Shichida, R. Needleman, J. K. Lanyi, M. Bizounok, J. Herzfeld, J. Raap, and J. Lugtenburg. 2000. Local and distant protein structural changes on photoisomerization of the retinal in bacteriorhodopsin. *Proc. Natl. Acad. Sci. U. S. A.* 97:4643–4648.
- Kimura, Y., D. G. Vassilyev, A. Miyazawa, A. Kidera, M. Matsushima, K. Mitusoka, K. Murata, T. Hirai, and Y. Fujiyoshi. 1997. Surface of bacteriorhodopsin revealed by high-resolution electron crystallography. *Nature.* 389:206–211.
- Kobayashi, T., M. Terauchi, T. Kouyama, M. Yoshizawa, and M. Taiji. 1991. Femtosecond spectroscopy of acidified and neutral bacteriorhodopsin. *Proc. SPIE-Int. Soc. Opt. Eng.* 1403:407–416.
- Kovacs, I., K. Hollós-Nagy, and G. Varó. 1995. Dark adaptation and spectral changes in Triton-X-100-treated bacteriorhodopsin. *J. Photochem. Photobiol. B.* 27:21–25.
- Krebs, M. P., W. Li, and T. P. Halambeck. 1997. Intramembrane substitutions in helix D of bacteriorhodopsin disrupt the purple membrane. *J. Mol. Biol.* 267:172–183.
- Landau, E. M., and J. P. Rosenbusch. 1996. Lipidic cubic phases: a novel concept for the crystallization of membrane proteins. *Proc. Natl. Acad. Sci. U. S. A.* 93:14532–14535.
- Lanyi, J. K. 1997. Mechanism of ion transport across membranes: Bacteriorhodopsin as a prototype for proton pumps. *J. Biol. Chem.* 272: 31209–31212.
- Lanyi, J. K. 1999. Progress toward an explicit mechanistic model for the light-driven pump, bacteriorhodopsin. *FEBS Lett.* 464:103–107.
- Lanyi, J. K., and G. Varó. 1995. The photocycle of bacteriorhodopsin. *Isr. J. Chem.* 35:365–386.
- Liu, S. Y. 1990. Light-induced currents from oriented purple membrane: I. Correlation of the microsecond component (B2) with the L-M photocycle transition. *Biophys. J.* 57:943–950.
- Logunov, S. L., M. A. El-Sayed, L. Song, and J. K. Lanyi. 1996. Photoisomerization quantum yield and apparent energy content of the K intermediate in the photocycles of Bacteriorhodopsin, its mutants D85N, R82Q, and D212N, and deionized blue Bacteriorhodopsin. *J. Phys. Chem.* 100:2391–2398.
- Logunov, S. L., T. M. Masciangioli, V. F. Kamalov, and M. A. El-Sayed. 1998. Low-temperature retinal photoisomerization dynamics in Bacteriorhodopsin. *J. Phys. Chem.* 102:2303–2306.
- Logunov, S. L., L. Song, and M. A. El-Sayed. 1994. pH Dependence of the rate and quantum yield of the retinal photoisomerization in Bacteriorhodopsin. *J. Phys. Chem.* 98:10674–10677.
- Logunov, S. L., V. V. Volkov, M. Braun, and M. A. El-Sayed. 2001. The relaxation dynamics of the excited electronic states of retinal in bacteriorhodopsin by two-pump-probe femtosecond studies. *Proc. Natl. Acad. Sci. U. S. A.* 98:8475–8479.
- Lozier, R. H., R. A. Bogomolni, and W. Stoeckenius. 1975. Bacteriorhodopsin, a light-driven proton pump in. *Biophys. J.* 15:955–962.
- Luecke, H., H.-T. Richter, and J. K. Lanyi. 1998. Proton transfer pathways in bacteriorhodopsin at 2.3 angstrom resolution. *Science.* 280: 1934–1937.
- Luecke, H., B. Schobert, H.-T. Richter, J.-P. Cartailier, and J. K. Lanyi. 1999a. Structural changes in bacteriorhodopsin during ion transport at 2 angstrom resolution. *Science.* 286:255–260.
- Luecke, H., B. Schobert, H.-T. Richter, J.-P. Cartailier, and J. K. Lanyi. 1999b. Structure of bacteriorhodopsin at 1.55 Å resolution. *J. Mol. Biol.* 291:899–911.
- Mathies, R. A., C. H. B. Cruz, W. T. Pollard, and C. V. Shank. 1988. Direct observation of the femtosecond excited-state cis-trans isomerization in bacteriorhodopsin. *Science.* 240:777–779.
- Mathies, R. A., S. W. Lin, J. B. Ames, and W. T. Pollard. 1991. From femtoseconds to biology: mechanism of bacteriorhodopsin's light-driven proton pump. *Annu. Rev. Biophys. Biophys. Chem.* 20:491–518.
- Milder, S. J., T. E. Thorgeirsson, L. J. W. Miercke, R. M. Stroud, and D. S. Kliger. 1991. Effects of detergent environments on the photocycle of purified monomeric bacteriorhodopsin. *Biochemistry.* 30:1751–1761.
- Muccio, D. D., and J. Y. Cassim. 1979. Interpretation of the absorption and circular dichroic spectra of oriented purple membrane films. *Biophys. J.* 26:427–440.
- Nuss, M. C., W. Zinth, W. Kaiser, E. Koelling, and D. Oesterheld. 1985. Femtosecond spectroscopy of the first events of the photochemical cycle in bacteriorhodopsin. *Chem. Phys. Lett.* 117:1–7.
- Oesterheld, D., and W. Stoeckenius. 1971. Rhodopsin-like protein from the purple membrane of *Halobacterium halobium*. *Nat. New Biol. (London).* 233:149–152.
- Pebay-Peyroula, E., G. Rummel, J. P. Rosenbusch, and E. M. Landau. 1997. X-ray structure of Bacteriorhodopsin at 2.5 angstroms from microcrystals grown in lipidic cubic phases. *Science.* 277:1676–1681.
- Petrich, J. W., J. Breton, J. L. Martin, and A. Antonetti. 1987. Femtosecond absorption spectroscopy of light-adapted and dark-adapted bacteriorhodopsin. *Chem. Phys. Lett.* 137:369–375.
- Polland, H. J., M. A. Franz, W. Zinth, W. Kaiser, E. Koelling, and D. Oesterheld. 1984. Optical picosecond studies of bacteriorhodopsin containing a sterically fixed retinal. *Biochim. Biophys. Acta.* 767:635–639.
- Polland, H. J., M. A. Franz, W. Zinth, W. Kaiser, E. Koelling, and D. Oesterheld. 1986. Early picosecond events in the photocycle of bacteriorhodopsin. *Biophys. J.* 49:651–662.
- Rammelsberg, R., G. Huhn, M. Luebben, and K. Gerwert. 1998. Bacteriorhodopsin's intramolecular proton-release pathway consists of a hydrogen-bonded network. *Biochemistry.* 37:5001–5009.
- Reynolds, J. A., and W. Stoeckenius. 1977. Molecular weight of bacteriorhodopsin solubilized in Triton X-100. *Proc. Natl. Acad. Sci. U.S.A.* 74:2803–2804.
- Rouso, I., E. Khachatryan, Y. Gat, I. Brodsky, M. Sheves, M. Ottolenghi, and A. Lewis. 1997. Microsecond atomic force sensing of protein conformational dynamics: implications for the primary light-induced events in bacteriorhodopsin. *Proc. Natl. Acad. Soc. U.S.A.* 97: 7937–7941.
- Scherrer, P., M. K. Mathew, W. Sperling, and W. Stoeckenius. 1989. Retinal isomer ratio in dark-adapted purple membrane and bacteriorhodopsin monomers. *Biochemistry.* 28:829–834.
- Schoelein, R. W., L. A. Penteanu, R. A. Mathies, and C. V. Shank. 1991. The first step in vision: femtosecond isomerization of rhodopsin. *Science.* 254:412–415.
- Sharkov, A. V., A. V. Pakulev, S. V. Chekalin, and Y. A. Matveets. 1985. Primary events in bacteriorhodopsin probed by subpicosecond spectroscopy. *Biochim. Biophys. Acta.* 808:94–102.
- Song, L., M. A. El-Sayed, and J. K. Lanyi. 1993. Protein catalysis of the retinal subpicosecond photoisomerization in the primary process of bacteriorhodopsin photosynthesis. *Science.* 261:891–894.
- Song, L., M. A. El-Sayed, and J. K. Lanyi. 1996. Effect of changing the position and orientation of Asp85 relative to the protonated Schiff base within the retinal cavity on the rate of photoisomerization in bacteriorhodopsin. *J. Phys. Chem.* 100:10479–10481.

- Song, L., D. Yang, M. A. El-Sayed, and J. K. Lanyi. 1995. Retinal isomer composition in some bacteriorhodopsin mutants under light and dark adaptation conditions. *J. Phys. Chem.* 99:10052–10055.
- Subramaniam, S., M. Gerstein, D. Oesterhelt, and R. Henderson. 1993. Electron diffraction analysis of structural changes in the photocycle of bacteriorhodopsin. *EMBO J.* 12:1–8.
- Varo, G., and J. K. Lanyi. 1991. Effects of the crystalline structure of purple membrane on the kinetics and energetics of the bacteriorhodopsin photocycle. *Biochemistry.* 30:7165–7171.
- Wang, J.-P., and M. A. El-Sayed. 2001. Time-resolved FTIR spectroscopy of the polarizable proton continua and the proton pump mechanism of bacteriorhodopsin. *Biophys. J.* 80:961–971.
- Wang, J.-P., C. D. Heyes, and M. A. El-Sayed. 2002. Refolding of thermally denatured bacteriorhodopsin in purple membrane. *J. Phys. Chem. B.* 106:723–729.
- Wu, S., and M. A. El-Sayed. 1991. CD spectrum of bacteriorhodopsin: best evidence against exciton model. *Biophys. J.* 60:190–197.
- Ye, T., N. Friedman, Y. Gat, G. H. Atkinson, M. Sheves, M. Ottolenghi, and S. Ruhman. 1999a. On the nature of the primary light-induced events in bacteriorhodopsin: ultrafast spectroscopy of native and C13=C14 locked pigments. *J. Phys. Chem. B.* 103:5122–5130.
- Ye, T., E. Gershgoren, N. Friedman, M. Ottolenghi, M. Sheves, and S. Ruhman. 1999b. Resolving the primary dynamics of bacteriorhodopsin, and of a 'C13:C14 locked' analog, in the reactive excited state. *Chem. Phys. Lett.* 314:429–434.
- Zhong, Q., S. Ruhman, M. Ottolenghi, M. Sheves, N. Friedman, G. H. Atkinson, and J. K. Delaney. 1996. Reexamining the primary light-induced events in bacteriorhodopsin using a synthetic C13:C14-locked chromophore. *J. Am. Chem. Soc.* 118:12828–12829.